A Puff-on-Cell Model for Computing Pollutant Transport and Diffusion[1]

C. M. SHEIH

Atmospheric Physics Section, Radiological and Environmental Research Division, Argonne National Laboratory, Argonne, Ill. 60439

(Manuscript received 4 June 1977, in final form 28 September)

ABSTRACT

A scheme is developed to minimize the pseudo-diffusion which arises in numerical solutions of finite-difference equations of turbulent diffusion and transport. In the present model, the subgrid scale distribution of the pollutant concentration is parameterized by a Gaussian puff. At each time step the concentration within each grid volume is characterized by a Lagrangian puff. The center of each Lagrangian puff is advected by the mean wind and its boundaries are expanded or contracted by diffusive displacements, computed from the values of concentration, atmospheric turbulent diffusivity, and the gradient of pollutant concentration between the adjacent grid volumes. The standard deviation of the puff is parameterized as a linear combination of the grid length and the diffusive displacement. The constants in the parameterization are determined by calibrating the standard deviation of the puff width predicted by the numerical model against that of an analytical solution. The pollutant is then distributed back to the surrounding Eulerian grid volumes, preserving the first and the second moments of the concentration distribution. The use of the model is illustrated by predicting the vertical concentration distribution of sulfur dioxide and sulfate for a period of 5 days. Furthermore, the requirement for realistic surface-layer parameterization in such numerical models is demonstrated by comparing the results of the constant-flux layer parameterization based upon the modern similarity theory with those of the conventional linear-profile approximation.

1. Introduction

Most finite-difference methods of modeling dispersion have been shown to introduce numerical pseudo-diffusion which can be much larger than the true diffusion in the fluid flow and can even generate negative values in the predicted pollutant concentrations (Bassett *et al.*, 1973). Two notable attempts to minimize the effect of pseudo-diffusion have been reported. Sklarew (1970) develops the particle-in-cell (PIC) method in which the pollutant concentration is specified by numerous particles, each particle representing a certain unit of the pollutant. The particles are tracked in a Lagrangian frame and their displacements during each time step are found by multiplying the time increment by the sum of the mean wind and diffusive velocities. The diffusive velocity is computed from the turbulent eddy diffusivity, the pollutant concentration, and the concentration gradients between adjacent grid volumes. The concentration in each grid volume is then calculated by dividing the total pollutant, represented by the particles present in the grid volume, by the grid volume.

Egan and Mahoney (1972) developed a different type of numerical scheme. At each time step, after computing the Lagrangian transport, they calculate the first and the second moments of the pollutant concentration distribution in each of the grid volumes. The moments are then used to construct a weighting function for distributing the pollutant from the Lagrangian grid volume to its surrounding Eulerian grid points, such that the first and the second moments remain the same after the distribution.

The present method replaces Sklarew's numerous particles in a grid volume by a puff and avoids the computation of the moments, as in the model of Egan *et al.*, by parameterizing subgrid-scale concentration with a Gaussian puff. In regard to the absence of a proper treatment of the numerical integration of surface layer in available pollutant transport models, a surface-layer parameterization based on a similarity theory has been assembled and combined with the present numerical scheme. As an example for the use of the method, the vertical distribution of sulfuric pollutant concentration for a long-range transport is simulated and the need for surface-layer parameterization has been demonstrated.

2. Description of the model

a. Theory

For simplicity in demonstrating the scheme, a one-dimensional diffusion equation will be used, i.e.

$$\frac{\partial C}{\partial t}+u\frac{\partial C}{\partial x}=\frac{\partial}{\partial x}\left(D\frac{\partial C}{\partial x}\right), \tag{1}$$

[1] Work supported by U. S. Energy and Research Development Administration.

where C is concentration, t is time, x is the spatial coordinate, u is the wind velocity (positive along increasing x), and D is eddy diffusivity. For an incompressible flow the above equation can be written as

$$\frac{\partial C}{\partial t}+\frac{\partial (u+\xi)C}{\partial x}=0 \tag{2}$$

with

$$\xi=-\frac{D}{C}\frac{\partial C}{\partial x}. \tag{3}$$

Eq. (2) implies that pollutant elements in the flow can be considered to be travelling in a Lagrangian frame with an effective velocity of $u+\xi$, as suggested by Sklarew (1970). Consequently, if a volume of pollutant originally corresponding to an Eulerian grid volume is followed in a Lagrangian frame, the total mass is conserved and the problems of numerical instability and negative concentration can easily be avoided. Fig. 1a shows the change experienced by the pollutant in a grid volume in a conventional model for each time step. The concentration in the shaded grid volume is uniform. For each time step the center of the grid volume is advected for a distance of $u\Delta t$ and the boundary of the grid volume is expanded by the diffusive velocities ξ^+ and ξ^- on the right and the left sides of the volume, respectively. In terms of a finite-difference, the diffusive velocities can be written as

$$\xi_i^+=\frac{D_i+D_{i+1}}{(C_i+C_{i+1})\Delta x}(C_i-C_{i+1}), \tag{4}$$

$$\xi_i^-=\frac{D_i+D_{i-1}}{(C_i+C_{i-1})\Delta x}(C_i-C_{i-1}). \tag{5}$$

The magnitude of the pseudo-diffusion is critically dependent upon the method which one chooses to distribute the pollutant in the displaced Lagrangian grid volume back to the original Eulerian grid system. Egan and Mahoney (1972) assume a uniform concentration distribution across the puff, compute the first and second moments of the Lagrangian grid volume, and then distribute the pollutant in the Lagrangian grid volume back to the Eulerian grid system in such a manner such that these moments of the Lagrangian grid volume are preserved. In addition to a uniform concentration distribution over the grid volume, other distribution functions capable of approximating their criteria could also be used. An obvious candidate is a Gaussian distribution function, which has the advantage that if one uses it as a weighting function to distribute the pollutant in the puff to its surroundings, it will automatically preserve the first and the second moments. Also the Gaussian distribution approaches an asymptotic distribution function of the pollutant in the Lagrangian volume if the time increment in the numerical integration becomes very large and if there

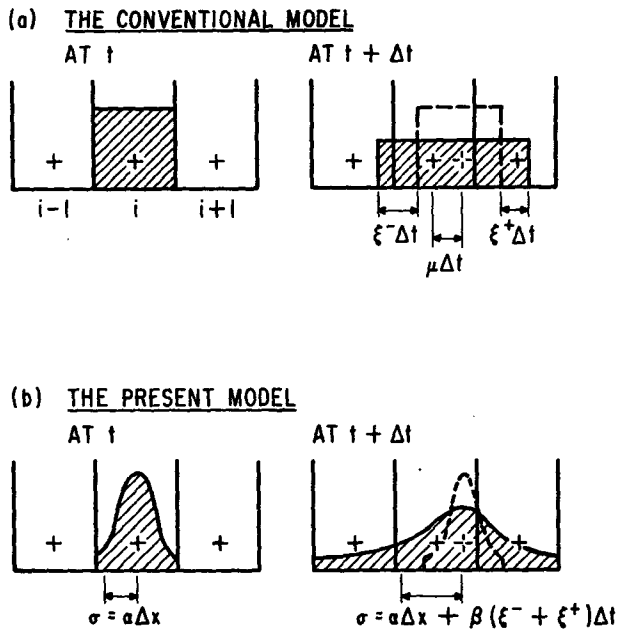

FIG. 1. Graphical representations of the transport processes of (a) conventional and (b) the present models. Dashed lines are advection without diffusion and shaded areas are total concentration distributions.

is no pollutant surrounding the Lagrangian volume. Fig. 1 (b) is a schematic representation of the present model. The distribution functions of the pollutant concentration in an Eulerian grid volume at the time t, denoted by a prime, and its Lagrangian counterpart at $t+\Delta t$ are parameterized in the following forms

$$P'(x_l,x_i)=\begin{cases}\exp\left\{-0.5\left[\dfrac{x_l-x_i}{\alpha\Delta x}\right]^2\right\} \\ \qquad\qquad \text{for } l=i-1,\ i \text{ and } i+1, \\ 0, \qquad \text{otherwise,}\end{cases} \tag{6}$$

$$P(x_l,x_i)=\begin{cases}\exp\left\{-0.5\left[\dfrac{x_l-(u\Delta t+x_i)}{\alpha\Delta x+\beta(\xi_i^++\xi_i^-)\Delta t}\right]^2\right\} \\ \qquad\qquad \text{for } l=i-1,\ i \text{ and } i+1, \\ 0, \qquad \text{otherwise,}\end{cases} \tag{7}$$

where $P'(x_l,x_i)$ and $P(x_l,x_i)$ represent the probability distributions of pollutant concentration in the Eulerian and the Lagrangian volume, respectively, at the x_l grid volume due to the pollutant in the x_i grid volume, α and β are constants relating the standard deviation of the Gaussian distribution to the grid length and the displacement due to diffusion. These constants will be determined by calibrating the model against the analytical solution of pollutant dispersion from a continuous point source in a uniform flow. The time increment Δt should be determined from the criterion that the

total displacement of a pollutant element in one time step is smaller than the grid length, i.e.,

$$(u+\xi)\Delta t<\Delta x. \tag{8}$$

This criterion is normally required to ensure computational stability in solving a finite difference equation. In the present model there is no stability problem involved, because the pollutant in each grid volume is tracked in a Lagrangian frame and is redistributed back to the Eulerian grid system at each time step which guarantees the conservation of the total pollutant in the flow. However, the constraint of Eq. (8) is necessary to satisfy the physical requirement that the parameters involved in the computation represent a close approximation to the local values. This constraint also simplifies computations by distributing the pollutant in the Lagrangian puff to only a few grid points, i.e., to the Eulerian grid point corresponding to the center of the Lagrangian position and to the adjacent grid point on either side. The pollutant concentration from the Lagrangian puff originated from the ith Eulerian grid is distributed according to the Gaussian weighting function to the Eulerian grid points $i-1$, i and $i+1$ by

$$\Delta C^{t+1}(x_l,x_i)=\frac{P(x_l,x_i)}{\sum_{j=i-1}^{i+1}P(x_j,x_i)}C^t(x_i),$$

$$\text{for } l=i-1,\ i \text{ and } i+1. \tag{9}$$

The final pollutant concentration at a point of interest x_l is simply the sum of the contribution from all the Lagrangian puffs, i.e.,

$$C^{t+1}(x_l)=\sum_{i=1}^{N}\Delta C^{t+1}(x_l,x_i), \quad \text{for } l=1,\ldots,N, \tag{10}$$

where N is the total number of Eulerian grid points.

Since the mean wind velocity should not affect the standard deviation of the Gaussian puff, α and β are independent of the mean velocity. Therefore, an Eulerian coordinate system moving with the mean velocity can be used to calibrate the numerical solution by comparing the result with the analytical solution. For the coordinate system moving with the mean velocity Eq. (1) is reduced to

$$\frac{\partial C}{\partial t}=\frac{\partial}{\partial x}\left(D\frac{\partial C}{\partial x}\right), \tag{11}$$

which is the equation governing the growth of a puff from an instantaneous source. The analytical solution of Eq. (11) for a constant D is

$$C(x,t)\approx(2Dt)^{-\frac{1}{2}}\exp\{-0.5[(x-x_0)/(2Dt)^{-\frac{1}{2}}]^2\}, \tag{12}$$

where x_0 is the coordinate of the center of the puff.

In order to test the numerical scheme, the growth of a one-dimensional puff under uniform atmospheric conditions is simulated. The parameters used are $u=0$ m s^{-1}, $D=10$ m^2 s^{-1}, $\Delta x=50$ m, $\Delta t=20$ s, and the total number of grid points is 41. The time increment is estimated from Eq. (8). The initial concentration distribution for the numerical integration is specified by Eq. (12) where the pollutant source is located at the center of the grid system and the proportionality constant is assumed to be unity. The results of the numerical prediction for various combinations of α and β are compared with the analytical solution. Fig. 2 shows the variance of the dimension of the puff at various time steps. The set $\alpha=0.5$ and $\beta=0.6$ gives the best approximation to the analytical solution. This set of values appears to be rather general because it also is applicable to other cases tested with various combinations of $u=10$ m s^{-1}, $\Delta x=25$ m, and $D=1$ m^2 s^{-1}, respectively. To demonstrate the effects of varying

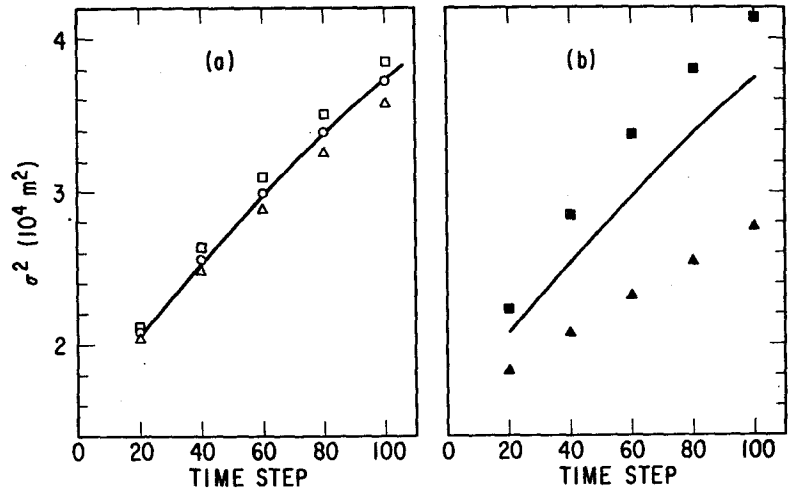

FIG. 2. Comparison of the puff variances of an analytical solution (solid lines) and the numerical predictions for the cases of $(\alpha, \beta)=(0.5, 0.6)$ (○), (0.5, 0.5) (△), (0.5, 0.7) (□), (0.4, 0.6) (▲) and (0.6, 0.6) (■).

each of the parameters, the figure is grouped into Figs. 2a and 2b, where α and β, respectively, are perturbed from their optimal values. The concentration profiles of the analytical solution and of the numerical prediction for the optimal values of α and β are compared in Fig. 3. Since the plume is symmetric about its center line, only half of the profiles are presented. The results indicate that the agreement is very good.

b. Extension to three-dimensional problems

To extend the method to a three-dimensional problem, let the coordinate axes be (x,y,z) and their corresponding indices, diffusive velocities, and mean wind velocities be (i,j,k), (ξ,η,ζ) and (u,v,w), respectively. The generalized diffusive velocities for 3-D components can be written as

$$S_m^+=\frac{D_m+D_{m+1}}{(C_m+C_{m+1})\Delta d}(C_m-C_{m+1}), \tag{13}$$

$$S_m^-=\frac{D_m+D_{m+1}}{(C_m+C_{m-1})\Delta d}(C_m-C_{m-1}), \tag{14}$$

for $(S,\Delta d,m)$ representing $(\xi,\Delta x,i)$, $(\eta,\Delta y,j)$ and $(\zeta,\Delta z,k)$. The probability distribution function corresponding to Eq. (7) will be

$$P(x_l,y_m,z_n;x_i,y_j,z_k)$$

$$=\begin{cases}\exp\left\{-0.5\left[\left(\dfrac{x-u\Delta t-x_i}{\alpha\Delta x+\beta(\xi_i^+ +\xi_i^-)\Delta t}\right)^2\right.\right. \\ \qquad +\left(\dfrac{y-v\Delta t-y_j}{\alpha\Delta y+\beta(\eta_j^+ +\eta_j^-)\Delta t}\right)^2 \\ \qquad \left.\left.+\left(\dfrac{z-w\Delta t-z_k}{\alpha\Delta z+\beta(\zeta_k^+ +\zeta_k^-)\Delta t}\right)^2\right]\right\} \\ \qquad \text{for } l=i-1,\ i \text{ and } i+1, \\ \qquad\quad m=j-1,\ j \text{ and } j+1, \\ \qquad\quad \text{and } n=k-1,\ k,\ k+1, \\ 0, \quad \text{otherwise.}\end{cases} \tag{15}$$

The amount of concentration distributed from the puff of (x_i,y_j,z_k) to the grid volume of (x_l,y_m,z_n) is

$$\Delta C^{t+1}(x_l,y_m,z_n;x_i,y_j,z_k)=P(x_l,y_m,z_n;x_i,y_j,z_k)$$

$$\times\Big[\sum_{q=i-1}^{i+1}\sum_{r=j-1}^{j+1}\sum_{s=k-1}^{k+1}P(x_q,y_r,z_s;x_i,y_j,z_k)\Big]^{-1}$$

$$\times C^t(x_i,y_j,z_k) \tag{16}$$

for $l=i-1$, i and $i+1$; $m=j-1$, j and $j+1$; and $n=k-1$, k and $k+1$. The predicted concentration at the end of a time step is

$$C^{t+1}(x_l,y_m,z_n)=\sum_{i=1}^{L}\sum_{j=1}^{M}\sum_{k=1}^{N}\Delta C^{t+1}(x_l,y_m,z_n;x_i,y_j,z_k) \tag{17}$$

for $l=1,\ldots,L$; $m=1,\ldots,M$; and $n=1,\ldots,N$, where (L,M,N) is the dimension of the grid system.

c. Numerical integration for the ground-level and the inversion height layers

The diffusion of pollutant near the surface of the ground is dominated by small-scale components of turbulence and can be simulated by finite-difference numerical methods only with an extremely small grid increment. This concept has been realized in modeling of meteorological variables by many investigators, such as Estoque (1960), Deardorff (1972), and Sheih and Moroz (1975) but has not yet been adopted in modeling of pollutant transport over urban areas (Egan and Mahoney, 1972; Sklarew, 1970; and Shir and Shieh, 1973). A promising approach to the problem is analytically integrating the flux-gradient relationships for the surface layer and expressing the surface flux or deposition velocity of a pollutant in terms of ground-surface features and the meteorological parameters in the atmosphere. This method gives explicit relationships for the concentration near the ground and the value at the top of the constant-flux layer predicted by numerical integration. Following this technique we shall set the first and the second grid points from the ground within the constant-flux layer where the analytical integration of the pollutant concentration is possible. Fig. 4 shows the coordinate system for the model. It should be noted that the coordinate axis x used earlier is for a generalized case, whereas z used in this section is the conventional symbol in meteorology for the vertical axis. Consequently, the results derived earlier are applicable to this section by replacing x with z. Fig. 4 shows that the grid increments are assumed to be constant except for the increment between z_1 and z_2; z_1 can be set at any arbitrary height within the constant-flux layer, because the concentration at this level can be computed from that of z_2 through the assumption of constant-flux layer and only enters into calculations in the predictive equation indirectly, as to be seen later. For this reason, the first grid volume is centered at z_2.

The procedures for the numerical integration of the pollutant concentration in the constant-flux layer is to compute the deposition velocity by using, for example, the equation given by Hicks (1974),

$$V_d(z)=\frac{ku(z)}{\left(\ln\dfrac{z}{z_0}-\psi_m\right)\left(\ln\dfrac{z}{z_p}-\psi_p\right)}, \tag{18}$$

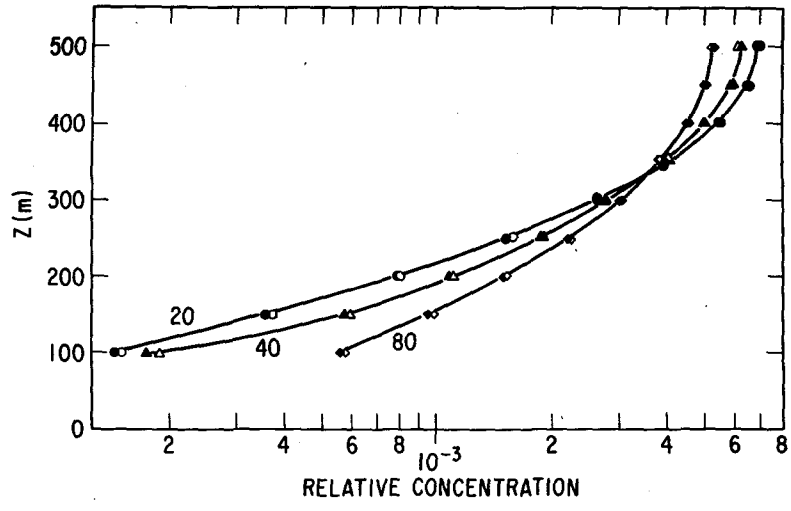

FIG. 3. Comparison of the concentration profiles of the analytical results (solid) and the numerical predictions (open) of the optimal case $(\alpha, \beta) = (0.5, 0.6)$ at various time steps.

where k is the von Kármán constant, z_0 and z_p are characteristic lengths for the transfer of momentum and pollutant over the ground surface, and ψ_m and ψ_p are the atmospheric stability parameters for momentum and the pollutant. The amount of pollutant taken away through surface deposition from the Lagrangian puff originated at z_2 is $V_d(z_2)\Delta t C(z_2)$. This reduces the total amount of the pollutant in the puff to $[\Delta z - V_d(z_2)\Delta t]C(z_2)$ which has to be distributed back to the Eulerian grid volume at z_2 and z_3 at the end of a time step, namely

$$\Delta C^{t+1}(z_l,z_2) = \frac{P(z_l,z_2)}{P(z_2,z_2)+P(z_3,z_2)}\left[1-\frac{V_d(z_2)\Delta t}{\Delta z}\right]C^t(z_2)$$

$$\text{for } l = 2 \text{ and } 3, \quad (19)$$

where the probability distribution function P can be computed from Eq. (7), once the following diffusive velocities

$$\xi_2^+ = \frac{D_2+D_3}{(C_2+C_3)\Delta z}(C_2-C_3), \quad (20)$$

$$\xi_2^- = \frac{D_2+D_1}{(C_2+C_1)\Delta z}(C_2-C_1), \quad (21)$$

are computed. It should be noted that C_1 enters into the computation indirectly in Eq. (21). Its value can be predicted through the relationship in the constant-flux layer, i.e.

$$C_1^{t+1} = \frac{V_d(z_2)}{V_d(z_1)}C_2^{t+1}. \quad (22)$$

One usually assumes no transport of pollutant across the inversion. This can be incorporated in the computation in the present model as

$$\Delta C^{t+1}(z_l,z_N) = \frac{P(z_l,z_N)}{P(z_{N-1},z_N)+P(z_N,z_N)}C^t(z_N)$$

$$\text{for } l = N-1 \text{ and } N. \quad (23)$$

Again, the probability distribution function P can be computed once the following diffusive velocities

$$\xi_N^+ = \frac{D_N}{\Delta z}, \quad (24)$$

$$\xi^- = \frac{D_N+D_{N-1}}{(C_N+C_{N-1})\Delta z}(C_N-C_{N-1}), \quad (25)$$

are calculated.

3. An Application of the model

The present numerical schemes were originally developed for computing the vertical concentration distribution for the pollutant transport and dispersion over the northeastern United States where unusually long periods of integration and stringent observance of the principle of the conservation of pollutant mass are required. The pollutant dispersion model used was suggested first by Durst *et al.* (1959) and applied later by Bolin and Persson (1975) to predict the transport of sulfur dioxide and sulfate over Western Europe. The model approximates the plume defined by an ensemble average of the trajectories of simulated tracers released from each pollutant source by a series of long-term average "puffs". Each puff is advected by the horizontal wind velocity averaged vertically from constant-flux to inversion height. Under this condition, the

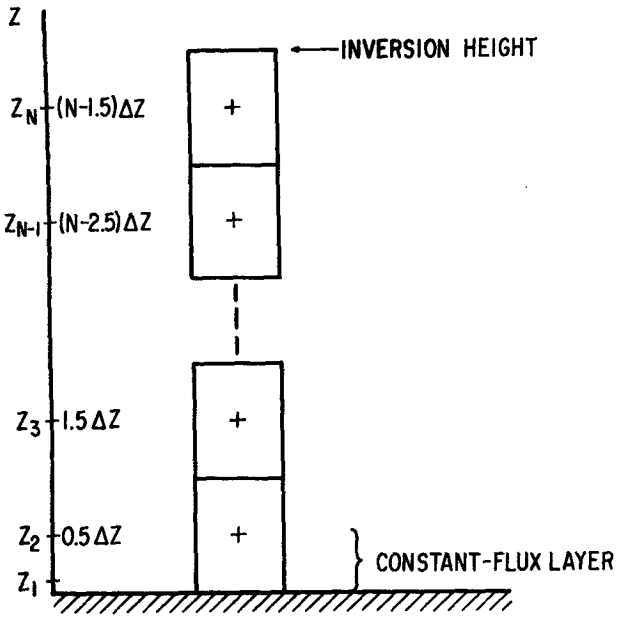

FIG. 4. Coordinate system of the model.

equations governing the vertical distributions of sulfur dioxide and sulfate in each puff have been approximated by (e.g., Eliassen and Saltbones, 1975)

$$\frac{\partial C_a}{\partial t}=\frac{\partial}{\partial z}\left(D\frac{\partial C_a}{\partial z}\right)-AC_a+\delta(z-h,t), \tag{26}$$

$$\frac{\partial C_b}{\partial t}=\frac{\partial}{\partial z}\left(D\frac{\partial C_b}{\partial z}\right)-BC_b+1.5AC_a, \tag{27}$$

where C_a and C_b are the concentrations of sulfur dioxide and sulfate integrated in the horizontal plane across the puff. Their units are gram per meter per gram of source. The decay constants for sulfur dioxide and sulfate are assumed to be $A=10^{-5}$ s^{-1} and $B=10^{-6}$ s^{-1}. The Kronecker delta function $\delta(z-h, t)$ represents a unit of sulfur dioxide released at the effective stack height h (200 m in this example). Results can be converted to the vertical concentration distributions for a particular source simply by multiplying C_a and C_b by the source strengths. The last term in Eq. (27) represents the formation of sulfate from the chemical transformation of sulfur dioxide. The eddy diffusivity is computed from the formula used by Bolin and Persson, i.e.

$$D=\begin{cases} ku_*z, & z_0\leqslant z\leqslant 85 \text{ m} \\ 85\ ku_*, & 85 \text{ m}<z<H \\ 0, & H\leqslant z \end{cases} \tag{28}$$

where $\kappa\approx 0.4$ is the von Kármán constant, and the friction velocity u_* and the inversion height H are assumed to be 0.4 m s^{-1} and 2 km, respectively. The commonly accepted deposition velocities at 2 m height of 1 cm s^{-1} for sulfur dioxide and 0.1 cm s^{-1} for sulfate are used. The roughness length z_0 is assumed to be 0.2 m. The grid spacing was shown earlier in Fig. 4 where $z_1=2$ m and $\Delta z=50$ m. Since Eq. (28) implies neutral stability, the stability parameters ψ_m and ψ_p are zero when Eq. (18) is used to compute the deposition velocity at z_2. The mean velocity $u(z)$ can be computed from the logarithmic wind profile with u_* and z_0 already given. The deposition velocity at z_2 is needed in Eq. (22) for predicting the pollutant concentration at the ground level. The time increment used is 20 s and the numerical integration is carried out for 120 h, which is estimated to be a typical time for the pollutant to travel across the west-east domain of interest.

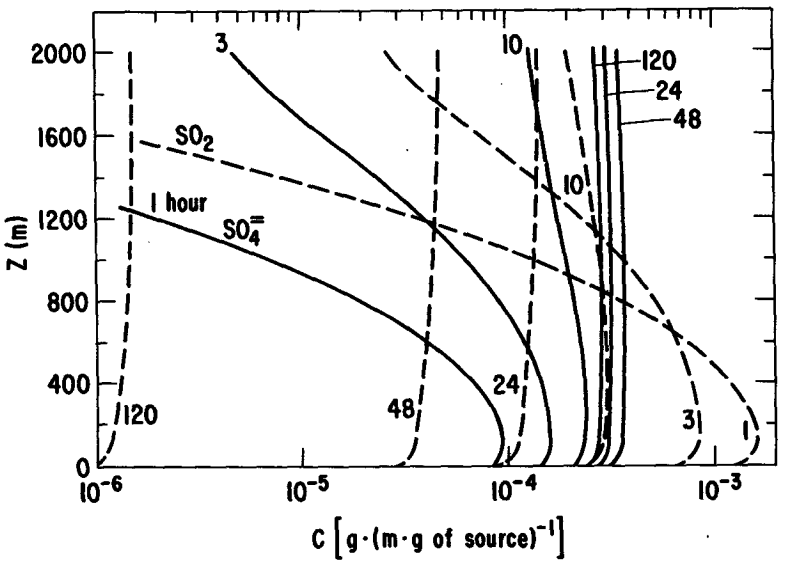

FIG. 5. Predicted vertical concentration profiles of sulfur dioxide (dashed) and sulfate (continuous) as function of time.

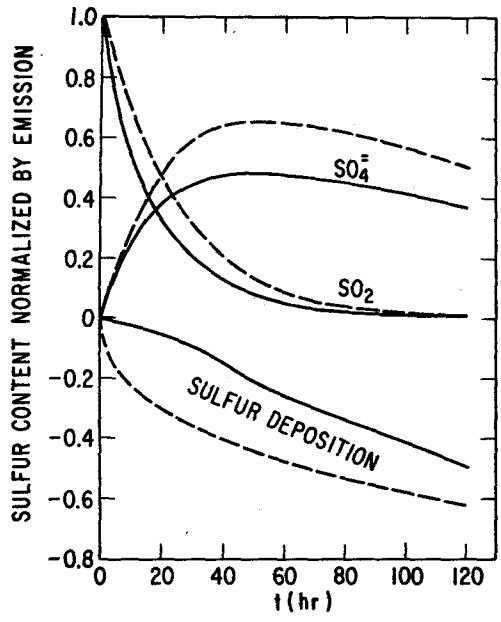

FIG. 6. Normalized sulfurs in the forms of sulfur dioxide, sulfate, and cumulative surface deposition as function of time. Solid and dashed lines are for the constant-flux parameterization and the conventional linear-profile approximation for the surface layer, respectively.

Fig. 5 shows the predicted concentration profiles which represent the values of concentrations integrated horizontally across the puff for sulfur dioxide and sulfate at various times after release. One hour after release the concentration of sulfur dioxide is still greatest near the stack height with a maximum value of 1.6×10^{-3} grams per meter per gram of pollutant source, and decreases rapidly to less than 10^{-4} above 1 km. The sulfur dioxide near the ground is gradually depleted by dry deposition at the surface and upward diffusion and consequently the maximum concentration appears at the inversion height after a day or so. The concentration of sulfur dioxide at human height (2 m) decreases from 1.3×10^{-3} at hour 1 to 10^{-6} at hour 120. On the other hand, the value of the entire concentration profile of sulfate is constantly increasing for 48 h after release. The value of the concentration at human height varies from 8.6×10^{-5} to 3.1×10^{-4} during this period. The concentration of sulfate reaches a quasi-equilibrium state two days after the release. The shape of the profiles remains almost the same and the value of the concentration decreases by less than 30% over the next three days.

In order to summarize the major implications of the results for sulfur pollution, the sulfur budgets at various times are presented in Fig. 6. Within the first 10 hours 53% of the sulfur dioxide has disappeared from the atmosphere through the chemical transformation to sulfate (25%) and surface deposition (23%). The total sulfate in the atmosphere reaches a maximum about two days after the release. The sulfur budgets at this time are made up of 9% sulfur dioxide, 48% sulfate and 43% surface deposition. At the end of 5 days, when the pollutant released in Illinois would be expected to reach East Coast areas, the sulfur budgets show 1% sulfur dioxide, 37% sulfates and 62% surface deposition.

To demonstrate the importance of the treatment of the surface layer parameterization, the current model has also been run with a conventional surface-layer treatment, in which the concentration at the first grid point is obtained by linearly interpolating between the concentrations at the second grid point and at the ground surface. The sulfur budgets for the conventional approach, represented by dashed lines, are compared with those of the present model in Fig. 6. It is seen that the conventional approach predicts significantly higher sulfur dioxide and sulfate concentrations in the atmosphere and less surface deposition. The largest

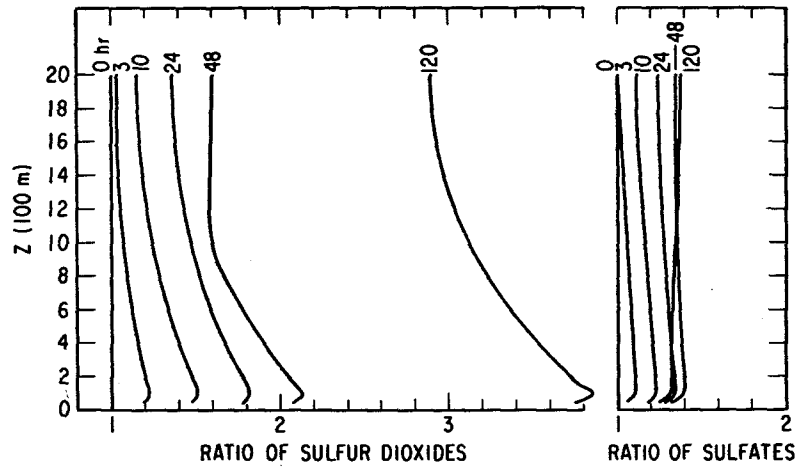

FIG. 7. The effect of surface-layer parameterization on the profiles of sulfur dioxide and sulfate: the values of the profiles are the concentration of the conventional approach divided by that of the constant-flux parameterization.

differences in sulfur budgets occurred around 35 h after release are 10, 16 and 26% of the sulfur emission, respectively.

The concentration profiles of the conventional method normalized by that of the constant-flux layer parameterization are shown in Fig. 7. The ratios of sulfur dioxide concentrations are larger than unity and increase with time. The maximum value of each profile, which occurs at 100 m, reaches 3.86 at 120 h from the release. The normalized sulfate concentrations increases at a much slower rate and for the region below 1 km also reaches a maximum at 100 m. These peak values increase to a maximum value of 1.4 at 48 h and decrease slightly thereafter. On the other hand, the normalized sulfate concentrations above 1 km increase monotonically and reach a quasi-steady state value of about 1.36 after 45 h.

It should be noted that the profiles below 50 m, not shown in Fig. 7, are in the constant-flux layer, in which the concentration profiles of the conventional and the constant-flux approximations vary linearly and logarithmically with height, respectively. For this reason the constant-flux approach of the represent model gives larger surface deposition as discussed earlier.

4. Conclusion

A puff-on-cell model has been developed to minimize pseudo-diffusion and ensure positive concentrations in the prediction of pollutant diffusion and transport with a finite-difference method. The unknown constants in the parameterization of the model are determined by calibrating the standard deviation of the puff width predicted by the numerical model with that of the corresponding analytical solution. Excellent agreement between the concentration profiles of the numerical prediction and the analytical solution is then obtained.

The model is used to predict, for a period of 5 days, the vertical concentration distributions of sulfur dioxide and sulfate resulting from a sulfur dioxide source at 200 m from the ground under typical meteorological conditions and chemical transformation rates. To address the question of the impact on East Coast areas of burning coal of high sulfur content in the Midwestern United States the numerical prediction with no precipitation scavenging being considered shows that 1% of the sulfur will be in the air in the form of sulfur dioxide, 37% in the form of sulfate and 62% of the emitted sulfur will be deposited on the ground en route.

Comparison between the approaches of the constant-flux parameterization based upon the modern similarity theory and the conventional linear-profile approximation for the surface layer shows that the apparent sulfur dioxide and sulfate concentrations in the atmosphere are higher for the conventional approach and the surface deposition is larger for the constant-flux method. The differences in terms of sulfur content reach maximum values of 10, 16 and 26% of the sulfur emission, respectively, around 35 h after the release.

Acknowledgment. Thanks are due to B. B. Hicks, G. D. Hess and J. D. Shannon for reviewing the manuscript. This work is supported by the U. S. Energy Research and Development Administration.

REFERENCES

Bassett, I. M., R. G. L. Hewitt and B. Martin, 1973: Design criteria for finite-difference models for eddy diffusion with winds that guarantee stability, mass conservation, and non-negative masses. *Mon. Wea. Rev.*, **101**, 528–534.

Bolin, B., and C. Persson, 1975: Regional dispersion and deposition of atmospheric pollutants with particular application to sulfur pollution over Western Europe. *Tellus*, **27**, 281–310.

Deardorff, J. W., 1972: Parameterization of the boundary layer for use in general circulation models. *Mon. Wea. Rev.*, **100**, 93–106.

Durst, C. S., A. F. Crossly and N. E. Davis, 1959: Horizontal diffusion in the atmosphere as determined by geostrophic trajectories. *J. Fluid Mech.*, **6**, 401–422.

Egan, B. A., and J. R. Mahoney, 1972: Numerical modeling of advection and dispersion of urban area source pollutants. *J. Appl. Meteor.*, **11**, 312–322.

Eliassen, A., and J. Saltbones, 1975: Decay and transformation rates of SO_2, as estimated from emission data, trajectories and measured air concentrations. *Atmos. Environ.*, **9**, 425–429.

Estoque, M. A., 1960: A theoretical investigation of the sea breeze. *Quart. J. Roy. Meteor. Soc.*, **86**, 523–534.

Hicks, B. B., 1974: Some micrometeorological aspects of pollutant deposition rates near the surface. Programs and Abstracts of Atmosphere-Surface Exchange of Particulate and Gaseous Pollutants—1974 Symposium, Richland, Wash., p. 29.

Sheih, C. M., and W. J. Moroz, 1975: Mathematical modeling of lake breeze. *Atmos. Environ.*, **9**, 575–586.

Shir, C. C., and L. J. Shieh, 1973: A generalized urban air pollution model and its application to the study of SO_2 distribution in the St. Louis metropolitan area. IBM RJ 1227 (No. 19588), IBM Thomas J. Watson Research Center, Yorktown Heights, N. Y. 10598.

Sklarew, R. C., 1970: A new approach: the grid model of urban air pollution. *J. Air Pollut. Control Assoc.*, **20**, 79.